Supplementary Information

Self-assembly of small molecules at hydrophobic interfaces using group effect

William Foster[1], Keisuke Miyazawa[2], Takeshi Fukuma[2], Halim Kusumaatmaja[1] and Kislon
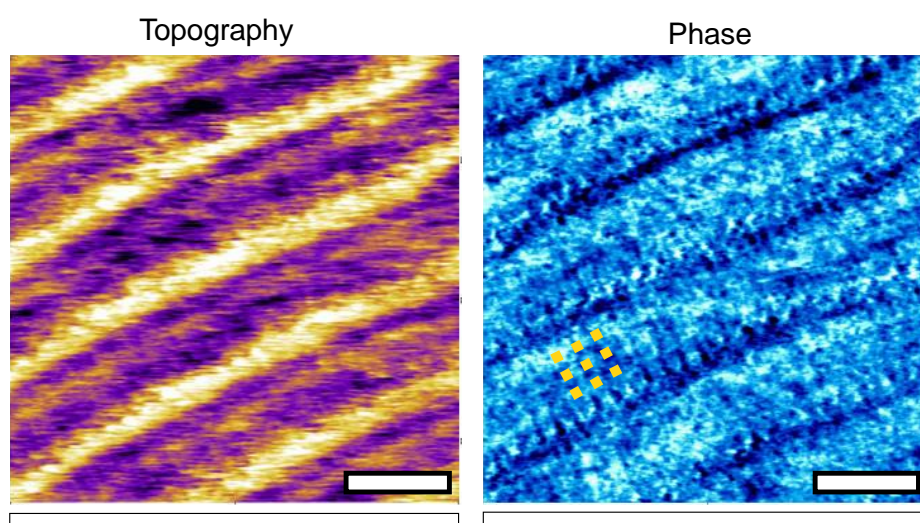
Voïtchovsky[1]*

[1]Durham University, Physics Department, Durham DH1 3LE

[2]Nano Life Science Institute (WPI-NanoLSI), Kanazawa University, Kanazawa, Japan.

* Corresponding Author: kislon.voitchovsky@durham.ac.uk

Content of the Supplementary Information:

- Supplementary Figures 1-12 with captions

- Supplementary references

Topography   Phase

Supplementary Figure 1: Substructures in basic monolayers formed in a methanol-water mixture. Phase images of structures in a 50:50 methanol water mixture reveal ångström-scale perpendicular sub-features (dashed yellow lines) corresponding to water and methanol molecules forming correlated parallel 'wires' on the surface of HOPG, consistent with observations in previous work[1,2]. The scale bar represents 5 nm. The blue scale bar represents a phase variation of 10°. The purple scale bar represents a topographic variation of 0.8 nm.
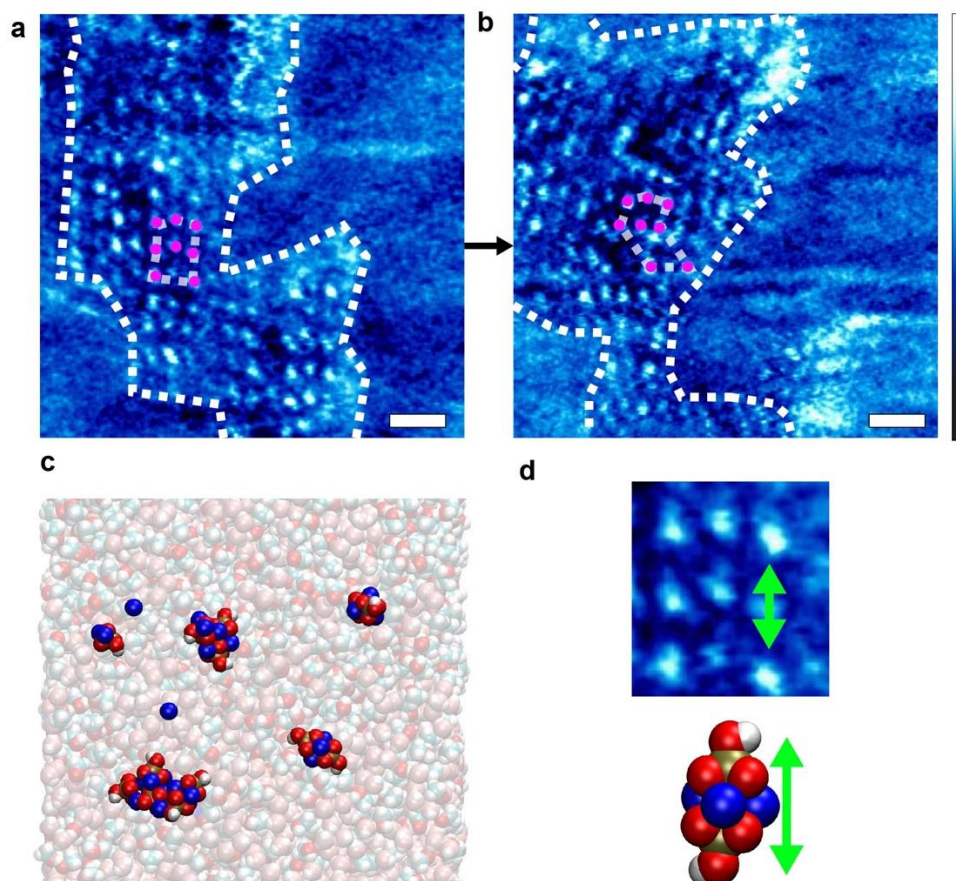
Supplementary Figure 2: High resolution images of some of the unique features observed in a methanol-disodium phosphate mixture. (a-b) The two consecutive images were taken within approx. 1 minute of each other. The pink dots denote example features (potentially molecules) that undergo a translational shift, indicating that the assembly is not stable under imaging conditions. The images are phase images for their better contrast. The scale bars represent 2 nm. The blue colour scale bar represents a phase variation of 12°. (c) MD simulations of Na^+ and HPO_4^{2-} ions in a 50:50 water-methanol mixture. The ions concentration corresponds to a weight percentage of 1%. The simulations demonstrate a tendency for the charged molecules to cluster together with their hydroxyl group facing outwards. The water and methanol molecules have been made partially transparent for better visibility of the Na^+ and HPO_4^{2-} ions. (d) The size of clusters involving 2 HPO_4^{2-} ions is comparable in size to the features observed in (a-b).

Details of the MD simulations: The simulations were performed using the molecular dynamics package GROMACS version 2016 [3]. The methanol molecules, sodium ions and HPO_4^{2-} ions were all described by the all atom OPLS force field[4]. The water was described by the TIP4P model[5]. Using this description for a system with Na_2HPO_4 in water with a weight percentage of 30% at 70°C gave a liquid density of 1203 kgm^{-3}, which is within 2.5% of the experimentally observed value (1232 kg m^{-3})[6]. The system was a NPT ensemble maintained at 298 K and 1 bar using a velocity rescale thermostat[7] and Parrinello-Rahman barostat[8,9] with coupling times of 0.5 ps and 1 ps, respectively. The simulation was performed with a 0.002 ps timestep. The mixture contained an equal number of water and methanol molecules as well as Na^+ and HPO_4^{2-} ions corresponding to a weight percentage of 1%. This is higher than would be the case for the 10 mM Na_2HPO_4 mixture studied in our experiments but can be justified by the limited size and timescale of the simulations. Furthermore, it has been shown that similar molecules tend to cluster together in aqueous solutions and the local concentration hence fluctuates[10]. Prior to analysis, the liquid box was equilibrated for 1 ns. Then a further 3 ns of simulations were performed during which we observed the behaviour of the Na^+ and HPO_4^{2-} ions. The snapshots were taken 1 ns into the run. At the end of the full 3 ns all of the charged molecules had clustered together. However, obtaining a meaningful average

cluster size for the concentrations studied in our experimental system is beyond computational feasibility due to the size of the simulation box.

Generally, highly charged molecules are difficult to simulate and can require force fields relying on quantum mechanical derivations[11–13]. We therefore compared our result with previously published results obtained for HPO_4^{2-} ions in a calcium diphosphate system, and which uses a force field derived specifically for phosphates[14]. The published study reports a similar effect where the HPO_4^{2-} ions form clusters with the hydroxyl groups facing outwards[10], consistent with our findings.
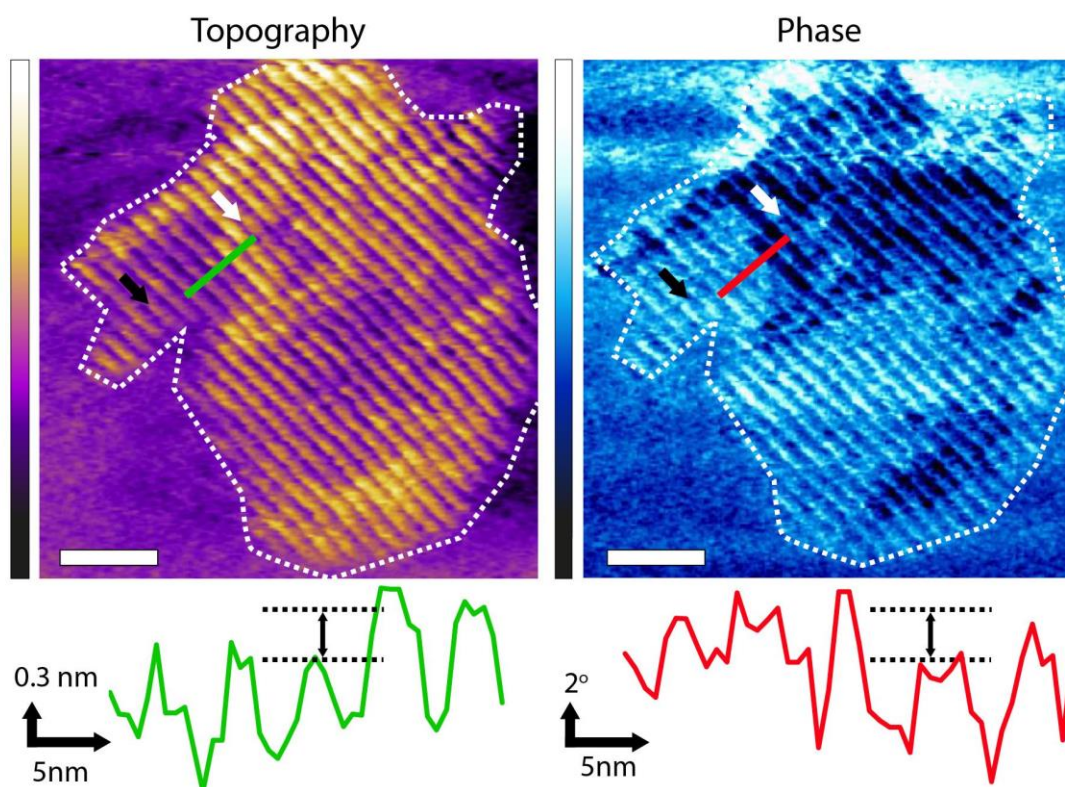

Supplementary Figure 3: Impact of disodium phosphate on the basic monolayers formed in a methanol-water mixture. The white and black arrows denote the two different parts of the monolayer, with the raised parts (white arrow) appearing on average 0.32 ± 0.06 nm higher than the surface of the basic monolayer (green topographic profile). This is identical to the effect observed in NaCl and KCl within error. The phase also shows a contrast between the two types of layer (red profile) The scale bar represents 25 nm. The purple scale bar represents a height variation of 1.5 nm. The blue scale bar represents a phase variation of 6°.

50:50 MeOH - NaCl
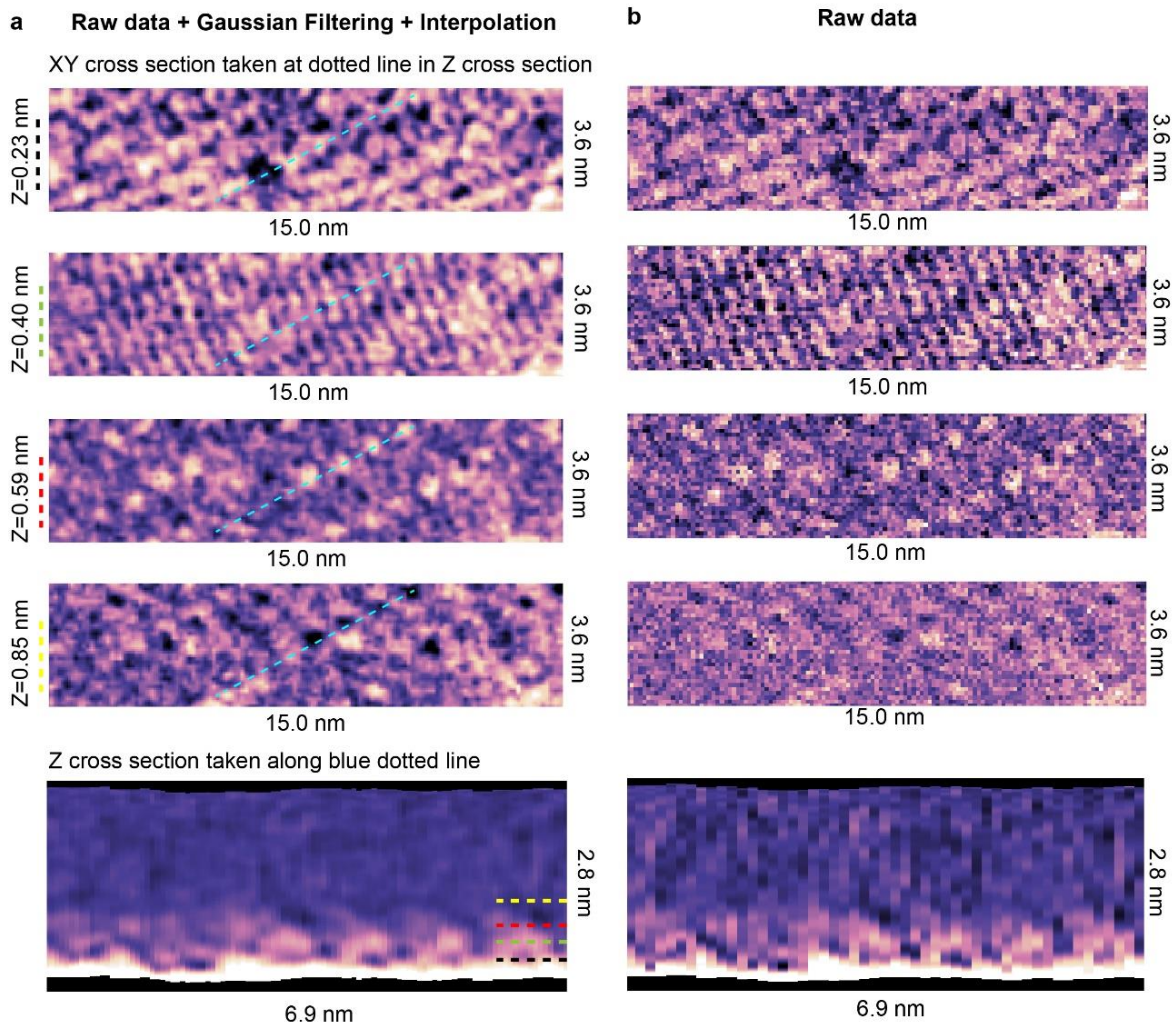

a Topography   Phase

b

c
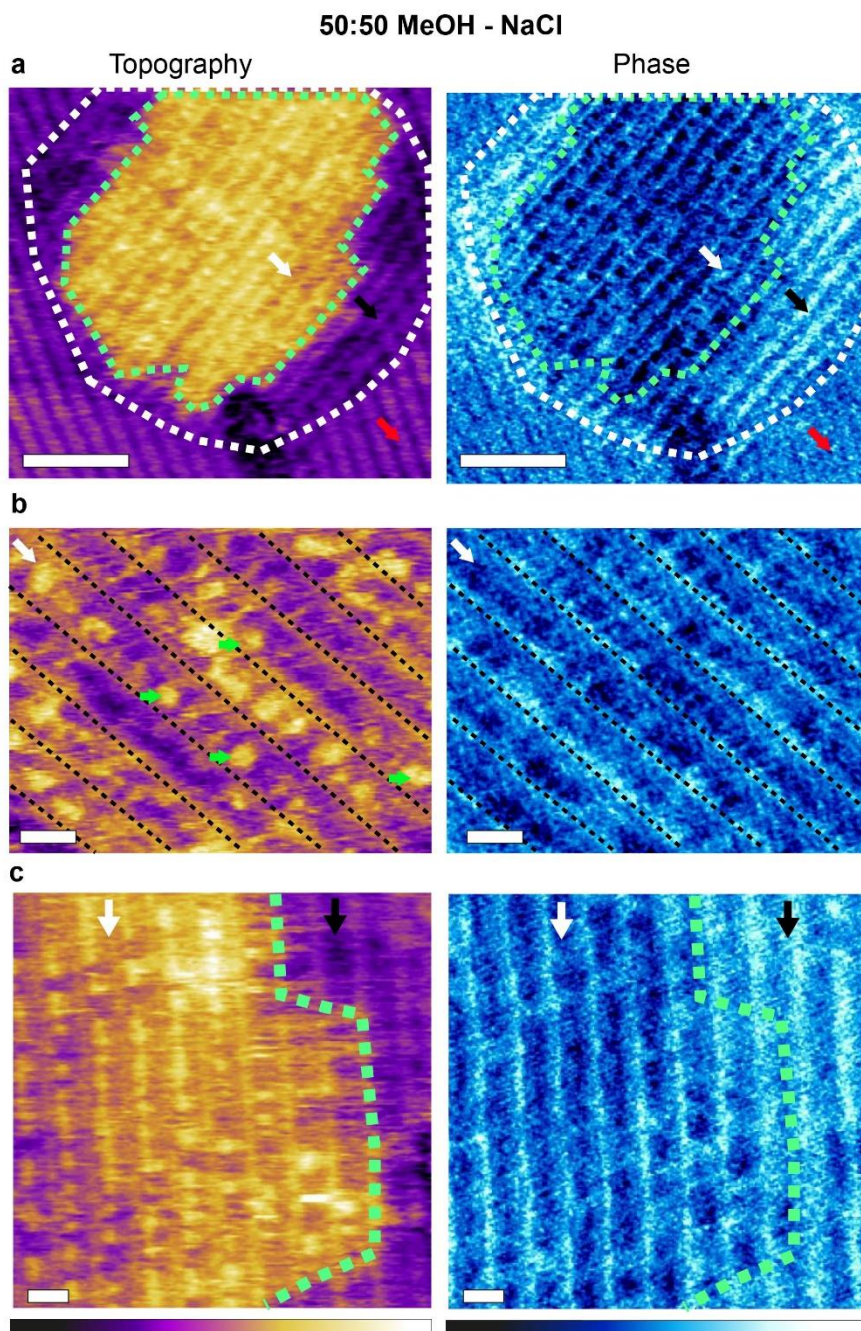
**Supplementary Figure 4: Impact of NaCl on the basic monolayers formed in a methanol-water mixture.** Topographic and phase images of raised areas formed in a 50:50 mixture of methanol with 137mM NaCl (a). The white and black arrows point to two different domains of a single structure (white dashed outline), with the green dashed line marking the boundary between the domains. The red arrow points to a region covered by the basic methanol-water monolayer unchanged by the presence of the salt ions. (b) High resolution images of the raised structures (white arrow) show small localised features sitting on top of the row structures and lying in registry with them (highlighted by the dashed black lines). The features are presumably molecular clusters involving the metal ions. (c) Some regions (black arrow) do not show any of these 'clusters', indicating standard basic methanol-water monolayer. The scale bar is 25 nm in (a), 5 nm in (b) and (c). The purple scale bar represents a height variation of 1 nm in (a) and 0.5 nm in (b-c). The blue scale bar represents a phase variation of 8° in (a) and (c) and 6° in (b). The direction of the patterns in (a-c) differ due to changes in the angle of scanning to obtain optimum resolution.
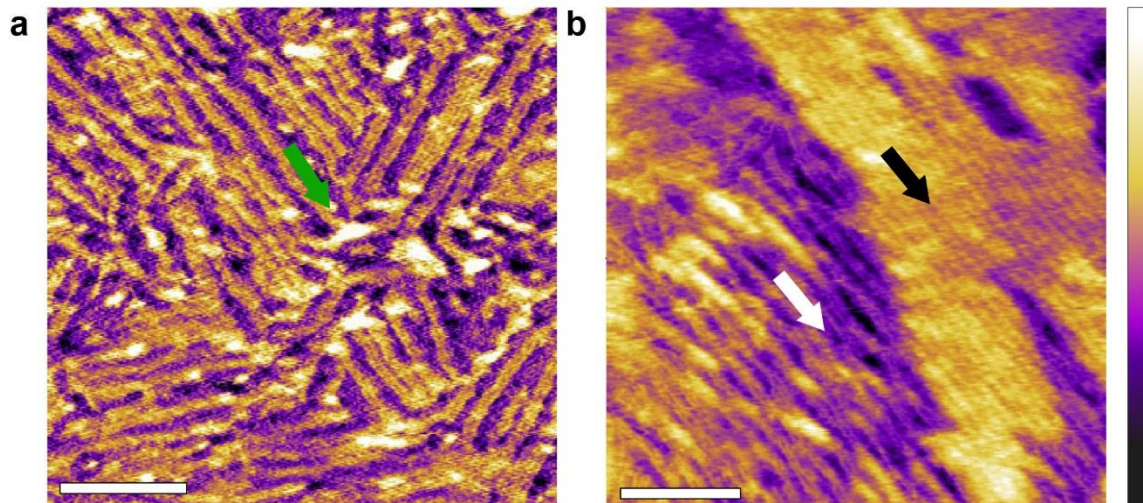
Supplementary Figure 5: High-resolution structures observed in a 50:50 methanol:PBS solution mixture. Distinct longitudinal structures with no well-defined periodicity are formed (a). Multiple round features (green arrow) can also be observed, likely due to the incorporation or clumping of the salt ions. Some regions (b) exhibit co-existence of PBS induced structures (white arrow) and structures resembling the basic methanol water monolayers (black arrow). The scale bars are 50 nm. The purple colour scale bar represents a height variation of 0.5 nm in (a) and 1 nm in (b).

a   **Raw data + Gaussian Filtering + Interpolation**   **b**   **Raw data**

XY cross section taken at dotted line in Z cross section

Z cross section taken along blue dotted line

Supplementary Figure 6: Details of the filtering and averaging procedure. The procedure is applied here on the set of measurements taken in the 5:95 methanol-PBS mixture and used in Fig. 3. (a) Shows the processed data after Gaussian filtering and interpolation procedures have been applied using a home-built software. The raw data is shown for comparison in (b). The images presented in Fig. 3c and d (main text) are then obtained by applying a further average filtering process that uses a pattern matching algorithm. Details of the algorithm are described elsewhere[15].
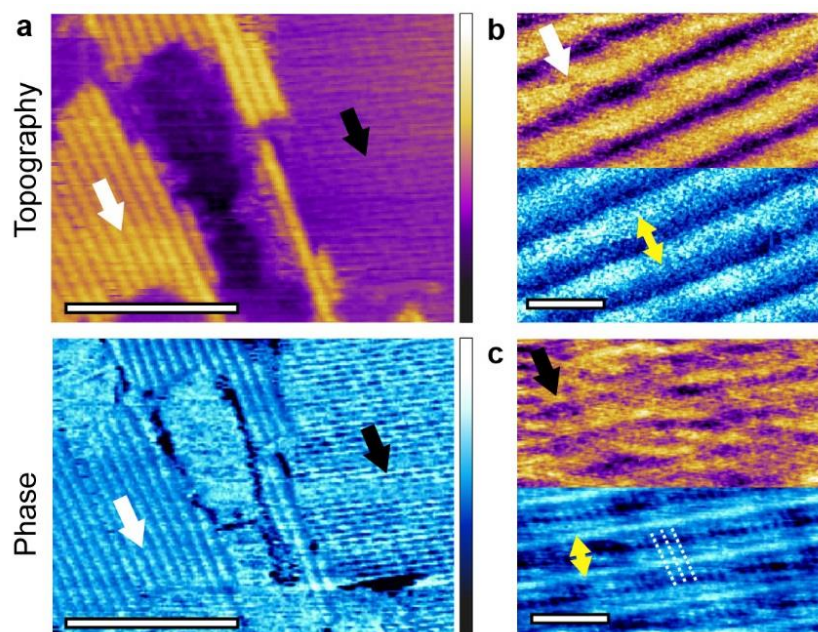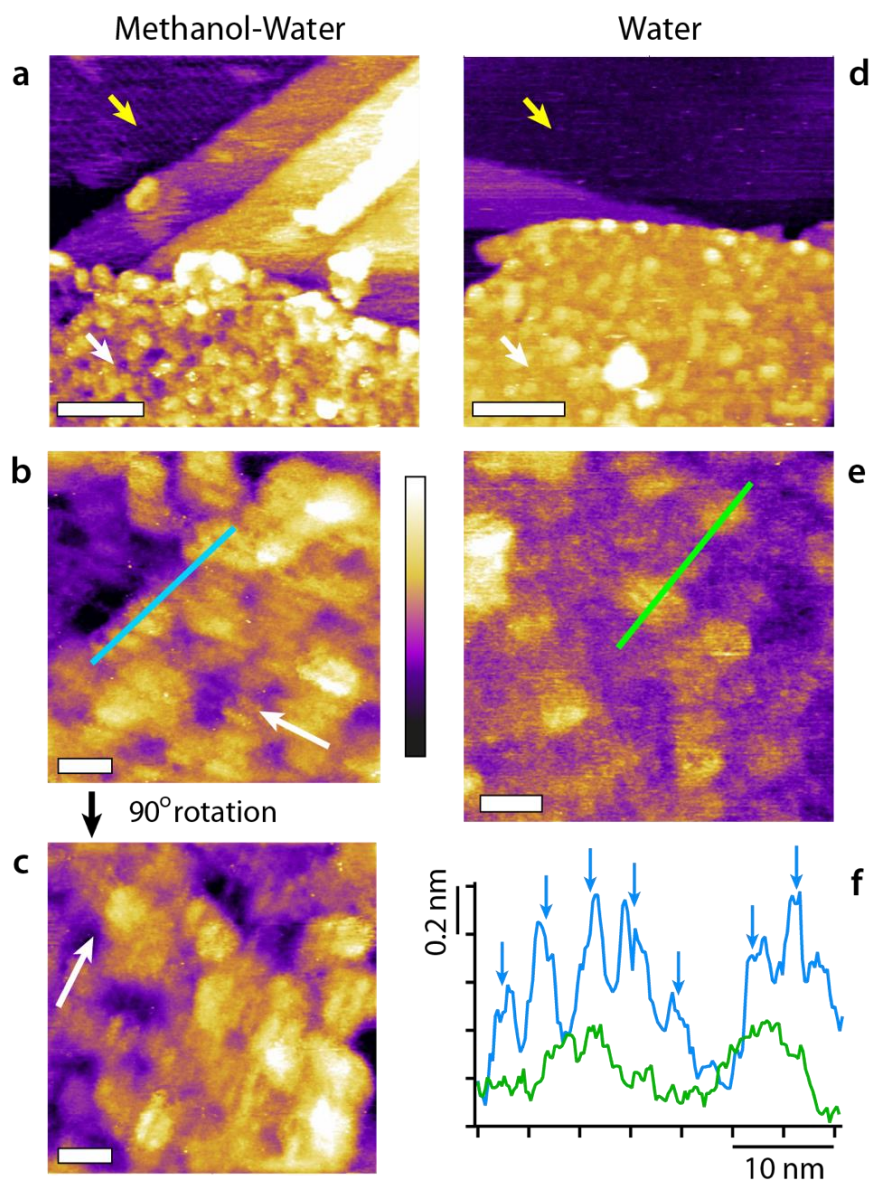
Supplementary Figure 7: High-resolution images of the HOPG 50:50 ethanol:water mixture interface. Co-existence of two types of ordered monolayers (a, black and white arrows) is visible. Higher magnification of the area highlighted with the white arrow in (a) reveals a basic structure with a periodicity of 5.40 ± 0.10 nm (b) but with no sub-features. In contrast, details of the area highlighted with the black arrow in (a) reveals a periodicity of 3.87 ± 0.10 nm with finer features running perpendicular to the main rows and spaced by 1.05 ± 0.10 nm (white dashed lines). The scale bars are 50 nm in (a) and 7 nm in (b) and (c). The purple scale bar represents a height variation of 3 nm (a), 0.5 nm (b), and 0.2 nm (c), and the blue scale bar represents a phase variation of (a) 6° (b) 1° and (c) 4°.
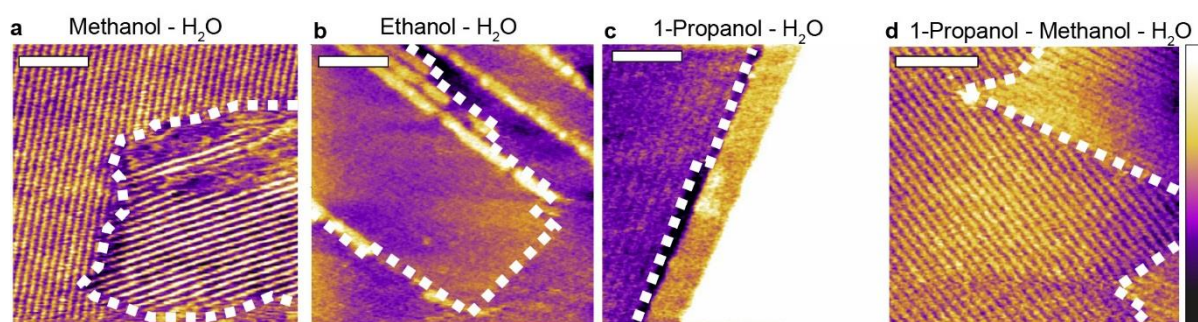

Supplementary Figure 8: Comparison between the interfacial supramolecular assemblies occurring in different mixtures of water and primary alcohols. The basic monolayer arrangement is visible in the 50:50 methanol:water mixture (a). In contrast, new domains with different periodicities, appearance and clear geometrical edges are formed in the 50:50 ethanol:water (b), 50:50 1-propanol:water (c) and 10:45:45 1-propanol-methanol (d) mixtures. This indicates that a different assembly has taken place. The scale bars are 45 nm. The colour scale bar represents a height variation of 0.5 nm in (a), (c) and (d) and 0.8 nm in (b).
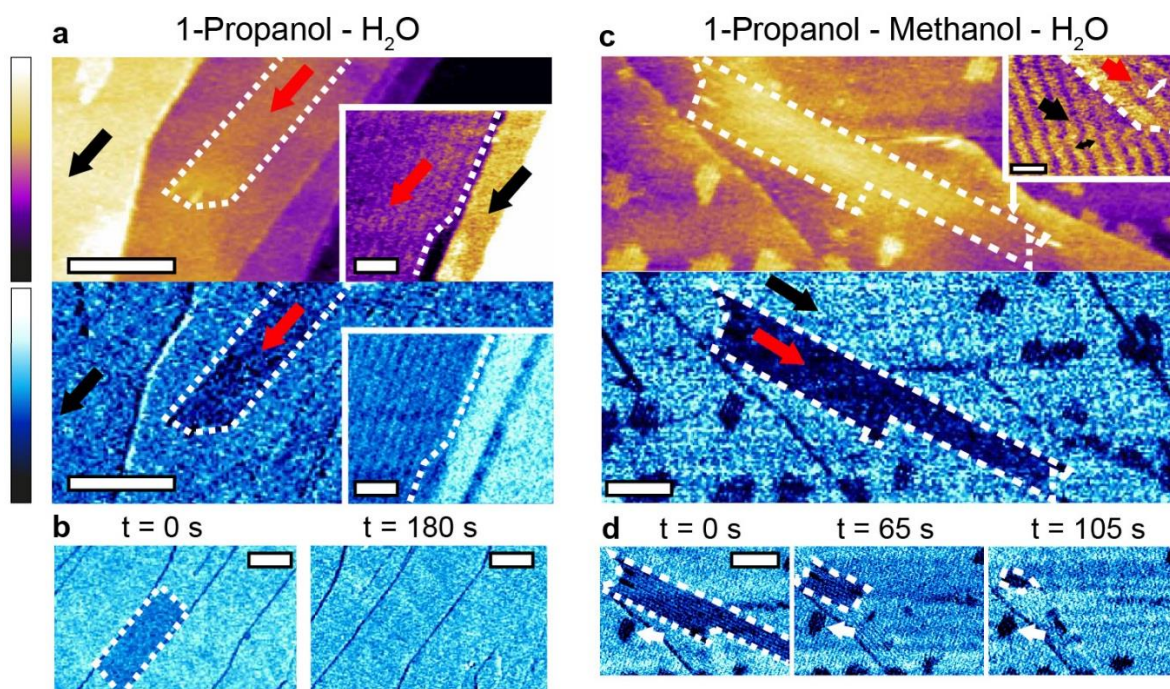
Supplementary Figure 9: Comparison between the interfacial supramolecular assemblies occurring in a binary 1-propanol-water mixture and a ternary 1-propanol-methanol-water mixture. The unique structures formed in a 50:50 1-propanol:water mixture (red arrows) exhibit similar properties to those formed in a 10:45:45 1-propanol-methanol-water mixture. The geometry of the structures in the binary mixture (a) strongly resemble that of certain motifs formed in the ternary mixture (c) and both motifs are unstable under imaging (b and d). Unlike the binary mixture, the presence of high quantities of methanol in the ternary mixture causes the rest of the surface to be covered in multi-layered structures resembling the basic methanol-water monolayers, indicating a co-existence of methanol and 1-propanol induced features. The scale bars represent 100 nm in (a) (b) and (c) main images, 20 nm and 10 nm in the insets of (a) and (c) respectively, and 50 nm in (d). The purple scale bar represents a height variation of 3 nm in (a) (0.6 nm in the inset) and 2 nm in (c) (0.4 nm in the inset). The blue scale bar represents a variation of 4° in (b) and 1.5° in (c) and (d).

Supplementary Figure 10: Comparison of the GrO in a methanol-water mixture and in pure water. At low resolution no differences are visible (a, d) but row-like structures become apparent in water-methanol at higher resolution, as can be seen in (b, c), where (c) is a subsequent image of the same area as (b) after the scanning direction has been rotated by 90°, confirming the features are not imaging artefacts. Such structures are not visible in pure water (e), confirmed by comparative profiles taken across the interface (f). The scale bars 50 nm (a, d), 10 nm (b, c, e). The height variation is 2 nm (a, d) and 0.8 nm (b, c, e).
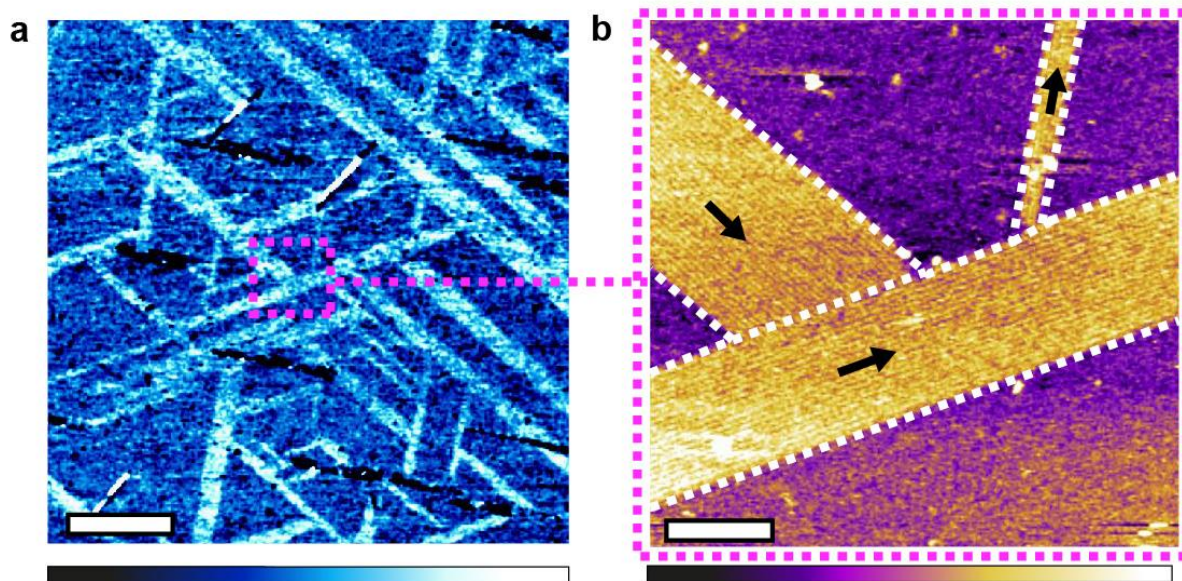
Supplementary Figure 11: Large scale image of self-assembled structures formed on MoS₂ in a 50:50 methanol water mixture. Elongated linear domains are clearly visible (lighter colours) in large scale phase images (a). The direction of growth reflects the hexagonal symmetry of the substrate, also visible in topography (b). Three domains have come into contact causing them to stop growing along their main axis. The scale bars represent 1 µm (a) and 100 nm (b). The blue scale bar represents a phase variation of 3° in (a). The purple scale bar represents a height variation of 0.6 nm in (b).
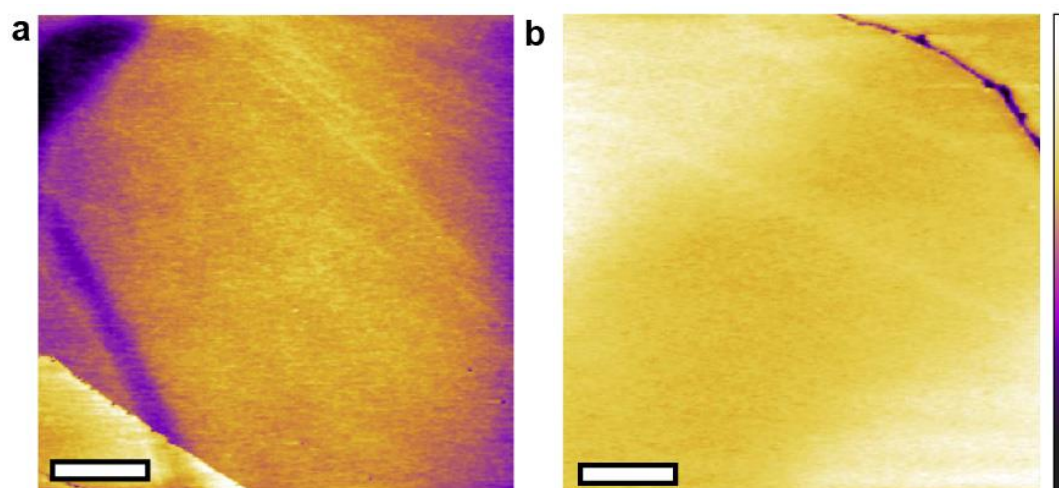
Supplementary Figure 12: AFM topographic images of MoS₂ in ultrapure water after 2 hours. No structures are visible at low (a) and higher resolution (b) in the absence of added alcohol. The scale bars represent 500 nm (a) and 100 nm (b). The purple scale bar represents a height variation of 1.5 nm in both.

Supplementary references

1   K. Voïtchovsky, D. Giofrè, J. J. Segura, F. Stellacci and M. Ceriotti, *Nat. Commun.*, 2016, **7**, 13064.

2   W. Foster, J. A. Aguilar, H. Kusumaatmaja and K. Voïtchovsky, *ACS Appl. Mater. Interfaces*, 2018, **10**, 34265–34271.

3   M. J. Abraham, T. Murtola, R. Schulz, S. Páll, J. C. Smith, B. Hess and E. Lindah, *SoftwareX*, 2015, **1–2**, 19–25.

4   W. L. Jorgensen, D. S. Maxwell and J. Tirado-Rives, *J. Am. Chem. Soc.*, 1996, **118**, 11225–11236.

5   J. L. Abascal and C. Vega, *J. Chem. Phys.*, 2005, **123**, 234505.

6   M. I. Nikandrov and Y. I. Mikhailov, *Russ. J. Appl. Chem.*, 2005, **78**, 1538–1539.

7   G. Bussi, D. Donadio and M. Parrinello, *J. Chem. Phys.*

8   M. Parrinello and A. Rahman, *J. Appl. Phys.*, 1981, **52**, 7182–7190.

9   S. Nosé and M. L. Klein, *Mol. Phys.*, 1983, **50**, 1055–1076.

10   G. Mancardi, C. E. Hernandez Tamargo, D. Di Tommaso and N. H. De Leeuw, *J. Mater. Chem. B*, 2017, **5**, 7274–7284.

11   L. Rao, Q. Cui and X. Xu, *J. Am. Chem. Soc.*, 2010, **132**, 18092–18102.

12   T. Dudev and C. Lim, *Chem. Rev.*, 2014, **114**, 538–556.

13   R. Qi, Z. Jing, C. Liu, J. P. Piquemal, K. N. Dalby and P. Ren, *J. Phys. Chem. B*, 2018, **122**, 6371–6376.

14   R. I. Ainsworth, D. Di Tommaso, J. K. Christie and N. H. De Leeuw, *J. Chem. Phys.*

15   K. Miyazawa, N. Kobayashi, M. Watkins, A. L. Shluger, K. I. Amano and T. Fukuma, *Nanoscale*, 2016, **8**, 7334–7342.